The Adaptive Optics and Transmit System for NASA's Laser Communications Relay Demonstration Project

Lewis C. Roberts Jr, Rick Burruss, Santos Fregoso, Harrison Herzog, Sabino Piazzolla, Jennifer E. Roberts, Gary D. sSpiers, and Tuan N. Truong

Jet Propulsion Laboratory, California Institute of Technology, 4800 Oak Grove Dr.,Pasadena CA 91109, USA

ABSTRACT

The Laser Communication Relay Demonstration is NASA's multi-year demonstration of laser communication to a geosynchronous satellite. We are currently assembling the optical system for the first of the two baseline ground stations. The optical system consists of an adaptive optics system, the transmit system and a camera for target acquisition. The adaptive optics system is responsible for compensating the downlink beam for atmospheric turbulence and coupling it into the modem's single mode fiber. The adaptive optics system is a woofer/tweeter design, with one deformable mirror correcting for low spatial frequencies with large amplitude and a second deformable mirror correcting for high spatial frequencies with small amplitude. The system uses a Shack-Hartmann wavefront sensor. The transmit system relays four beacon beams and one communication laser to the telescope for propagation to the space terminal. Both the uplink and downlink beams are centered at 1.55 microns. We present an overview of the design of the system as well as performance predictions including time series of coupling efficiency and expected uplink beam quality.

Keywords: Laser Communication, Adaptive Optics

1. INTRODUCTION

The Laser Communications Relay Demonstration (LCRD) project is NASA's multi-year demonstration of laser communication between multiple ground stations and a geosynchronous satellite. LCRD will provide two years of high data rate optical communications in an operational environment, demonstrating that optical communications can meet NASAs growing need for higher data rates while also enabling lower power, lower mass communications systems on spacecraft. In addition, LCRDs architecture will serve as a developmental test bed for additional methods, including symbol coding, ranging, link layer protocols, and network layer protocols.[1] LCRD will serve as a test bed for future NASA missions including the development of a future Advanced Telecommunications and Data Relay Satellite Service.[2] The mission is led by Goddard Space Flight Center (GSFC) with the participation of Massachusetts Institute of TechnologyLincoln Laboratory (MITLL), and Jet Propulsion Laboratory (JPL).

The LCRD space terminal will be a hosted payload on the U.S. Air Force's Space Test Program Satellite-6 (STPSat-6) in geosynchronous orbit. The space terminal is capable of simultaneously communicating with two ground stations. There are currently two optical ground stations. The primary ground station is located at JPL's Table Mountain Observatory in Wrightwood California.[3] It will use the 1-m Optical Communication Telescope Laboratory (OCTL) telescope.[4] The second ground station will be in Hawaii and will use a 0.6m receive telescope and a 0.15m transmit telescope.[5]

Optical Ground station 1 (OGS1) consists of multiple systems including the existing OCTL telescope, the communication and beacon lasers, the monitor and control system, laser safety and the the Integrated Optical System (IOS), which is the subject of this paper. The IOS system has two major functions. The first is to relay the received light from the telescope to the ground modem's single mode fiber. Its second function is relay light from the beacon and communication lasers to the telescope. Section 2 discusses the receive system, and Section 3

Further author information: (Send correspondence to L.C.R.)
L.C.R.: E-mail: lewis.c.roberts@jpl.nasa.gov

discusses the transmit system. The software that controls both elements is described in Section 4. Then Section 5 discusses the status of the project and what lies ahead. Finally Section 6 provides a quick summary of the paper.

2. RECEIVE SYSTEM

A number of requirements were levied on the IOS. Of those, three drive the complexity of the system. As the exact location of the host satellite was unknown until recently, the IOS is required to operate at elevation angles as low as 20°. Recently the satellite location was specified to be between 112-120° with a target of 107°. This puts it at an elevation angle of 50° for OGS1. The system is also required to work at the median seeing conditions at the Table Mountain, or a Fried's parameter of 5.2 cm measured at zenith at a wavelength of 500 nm. Finally the system was required to work day or night. Under these conditions the IOS is required to produce a coupling efficiency of 55%, which translates to a Strehl ratio of roughly 70%. The nominal received power levels will be 125nW/m^2 at the front of the IOS.

LCRD will use two communication modulations, Differential Phase Shift Keying (DPSK) and (Pulse-position modulation) PPM. DPSK requires a coherent signal, which is created by using a single mode fiber. Adaptive Optics (AO) is required on the receive system because atmospheric turbulence will broaden the incoming beam enough that very little of the light would be coupled into the fiber. PPM does not require a coherent signal and can use a focal plane array as its detector, but our modem uses the same single mode fiber for both PPM and DPSK.

AO is a technique where a deformable mirror is used to correct aberrations in the wavefront. These aberrations are sensed by a wavefront sensor (WFS). There are multiple types of wavefront sensors, each with its own advantages and disadvantages. For the IOS, we chose a Shack-Hartmann sensor in a Fried geometry. We carried out a trade study including several alternative types such as a phase-shifting Zernike sensor,[6] which is very promising, but has a low technology readiness level. The study also looked at self referencing interferometers (SRI),[7] which are immune to scintillation, but require more downlink power than is available to the IOS. Also, with a minimum elevation angle of 20°, scintillation is not expected to be a significant problem.

Most astronomical AO systems make their wavefront sensing measurements at one wavelength, and correct at another wavelength. For laser communication, where there is only a single incoming wavelength, we have to divert part of the incoming light to the WFS. The IOS has a baseline diversion of 20%, but we are reevaluating that based on the newly determined location of the satellite. The LCRD downlink wavelength is 1545 nm. The speed of the WFS measurement is critical for the AO system to keep up with the rapidly changing atmospheric turbulence conditions at the required 20° elevation and nominal r_0 of 5.2 cm. Our models have shown that we need to have frame rates on the order of 10 kHz to achieve our desired level of performance in the specified atmospheric conditions. The WFS camera is an off the shelf Xenics Cheetah InGaAs camera. Each lenslet in the WFS will illuminate an array of 2×2 detectors on the WFS focal plane array.

We carried out a trade study on the number of actuators across the primary. A higher actuator density will reduce the wavefront fitting error, but the WFS will have fewer photons per lenslet to make the wavefront measurements, which will increase the wavefront measurement error. In the end, we decided that 28 actuators across the primary mirror diameter would produce the best trade off between fitting error and measurement error. This lead us to the choice to use a Boston Micromachines 32×32 actuator Kilo MEMS DM[8] with a continuous facesheet. This DM only has an actuator stroke of 1.5 μm, which in turn drives us to use a woofer/tweeter design using the Boston Micromachines 12×12 actuator 3.5 μm stroke Multi-DM in addition to the Kilo DMs. Our current stroke budget shows that we need 3.1 μm of stroke for the required 20° elevation angle, which gives us 12% margin. For the actual elevation angle of 50°, we will have 23% margin. In a woofer/tweeter design, a Low Order DM (LODM) correcting low spatial frequencies, large amplitude aberrations and a High Order DM (HODM) correcting high spatial frequencies, small amplitude aberrations. MEMS DM have two advantages over conventional DMs. They are much smaller in diameter, on the order of 1 cm, which allows the rest of the optical train to be smaller. This reduces the cost of the optical train. Also the DMs themselves cost less than conventional DMs.

The IOS will be located in the coudé room of the OCTL facility. This room allows for multiple experiments to be set up simultaneously; a flat mirror on a rotation stage directs the optical beam to the desired experiment. The IOS will be located on a standard optical bench, and will be isolated from the room atmospheric turbulence with an enclosure that also blocks stray laser light from leaving the optical bench. The IOS components are mounted on four separate breadboards which are mounted on the optical bench, which is shown in Figure 1 Having the IOS mounted on separate breadboards facilitates moving the system from the development laboratory to the telescope. Also, the WFS and a portion of the transmit system are aligned separately.

In the following description, we trace the light going through the receive system as it comes from the telescope. The description starts at the Transmit/Receive Dichroic. In Figure 1, this is where the red line intersects the blue line. First the beam hits acquisition camera pickoff. A portion of the light gets diverted to a camera that images the uncompensated light. This is used to acquire the target and then to measure the Fried's parameter at 1 Hz. Next the light encounters the first of five off-axis parabola (OAP1) mirrors, which forms a pupil on the fast steering mirror (FSM). Then the downlink beam encounters OAP2 and OAP3, which form a second pupil on the HODM. The beam then encounters OAP4 and OAP5 which form a third pupil on the LODM. The next optic is a pair of filters that block any back scattering from the uplink beam from entering the downstream sensors. The wavefront sensor picks off 10% of the light with a beamsplitter. Another 10% of the light is picked off for the scoring camera. Then the light is coupled into the single mode fiber that goes to the ground terminal. The AO system takes up a much of a fairly large optical bench. Long focal length OAPs were used to ease the alignment; for other applications the system could be made much more compact.

The system also has an atmospheric turbulence simulator (ATS). A mirror can be slid into the beam path to inject light from the ATS into the AO system. The beam has the same optical properties as the downlink from the telescope and forms pupil images at the same locations. The ATS consists of two spinning phase plates with computer controlled rotation rates to simulate a variety of turbulence conditions.[9] The ATS will allow the IOS AO system to be tested in the lab over a wide variety of atmospheric conditions. This will improve the quality of the AO system, so that it will farther down the development path when it gets to the telescope. It can also be left on for several days to help find bugs that will impair operations. Doing this in the laboratory is much more efficient than doing it at the telescope saving time and labor costs. The telescope is a limited resource and can be closed due to inclement weather. Also, specific atmospheric conditions are not available on demand, but depend on the whim of nature. During operations the ATS will be used for regression testing when the system is started up. The performance on these standardized tests will allow us to track IOS performance over the course of the mission and hopefully detect failing components before they totally fail.

As mentioned above, a portion of the downlink beam is diverted to the scoring camera. The scoring camera produces an image of the compensated downlink beam. This is used to judge the quality of compensation by measuring the Strehl ratio. The IOS also receives a measurement of the received power in the modem, but that is slightly delayed and is also not available before the launch of the space terminal. The scoring camera is also used to measure the non-common path aberrations in the system using the Modified Gerchberg-Saxton algorithm.[10] The aberrations, which are not sensed by the WFS, can then be corrected by the DMs leading to improved image quality.

2.1 Performance Predictions

We made performance predictions based on the AO error budget.[11] Strehl ratio, or image quality is the usual metric used to judge AO performance, but for optical communication what matters is how much light gets coupled into the detector, in our case a single mode fiber. The metric for that is coupling efficiency and defined as the fraction of the light immediately before the fiber that gets coupled into the fiber. In Figure 2 we show the coupling efficiency as a function of Fried's parameter over the range of elevation angles that the space terminal could have been placed. As mentioned above, we recently have found out that it will be placed in the most optimal location. For the required 20° elevation, the system would have met it's requirements of 55% coupling efficiency, but for the current 50°, we will have plenty of margin.

While error budgets provide good insight into system performance, they assume constant proprieties of the atmosphere. To understand the temporal behavior of the system, we simulated time series of the coupling efficiency of the system using a wave optics simulation code based on FFT-based propagation and FFT-based

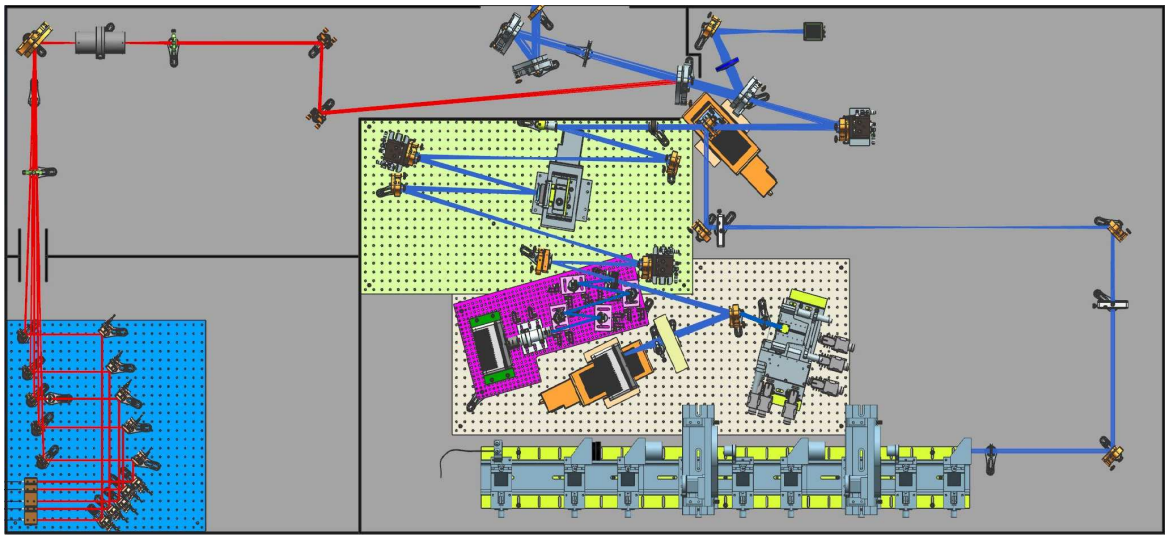

Figure 1. The IOS opto-mechanical layout. The transmit arm is marked in red, and the AO arm in blue. The WFS is mounted on the purple breadboard. The remaining components in the AO arm are divided between the tan and green breadboards. Much of the transmit system is mounted on the blue bread board on the left. The Atmospheric Turbulence Simulator (ATS) is at the bottom of the layout.

phase screen generation. Five Kolmogorov turbulence layers were used for the simulations. Long simulation run times are enabled by slowly breaking the frozen flow hypothesis and adding a small component of a new Kolmogorov phase screen at each time step. The simulations were run for two cases both at an elevation angle of 20°. The first case was with nominal atmospheric conditions for Table Mountain of $r_0 = 5.2$ cm and a ground layer wind speed of 2.3 m/s. The second case was for conditions at 90% of the cumulative distribution function: $r_0 = 2.7$ cm and a ground layer wind speed of 5.3 m/s. In both cases, the wind profile used was the San Diego wind profile for the month of January.[12] This wind profile is the average of decades of twice daily radiosonde launches and was the nearest launch site to Table Mountain. The wind direction was set to be transversal to the line of sight. The simulation produced 10 runs with a duration of one second each for both conditions. The sampling rate was 10 kHz. The coupling efficiency time series is plotted in Figure 3. The plot includes two consecutive 1 sec runs for the nominal conditions and for the 90th percentile case. At the higher wind speed and lower Fried parameter, the performance is more variable and produces a lower coupling efficiency. For the nominal case, the coupling efficiency is always above the required 0.55 value, while for the 90th percentile case, the average is just below the required level and sometimes much lower. This will result in degraded communication rates.

3. TRANSMIT SYSTEM

The ground station needs to transmit multiple lasers to the space terminal. These include the communication beam, and multiple beacon beams. There are multiple beacon beams so that they have different paths through the atmosphere and do not experience scintillation and phase aberrations at the same time, which provides a more consistent beam profile at the space terminal. The beacon beams allow the space terminal to identify the locaiton of the ground station and properly direct its communication beam at the ground station. The transmit system relays four beacon beams at a wavelength of 1553 nm to the telescope. They form overlapping beams with a divergence of 280 μrad on the sky. This beam width was set to match the spacecrafts location uncertainty. This eliminates the need to scan the sky with the beacon lasers and speeds the acquisition process. Each beacon laser has a average power of 2.5 W.[3] The acquisition camera has a field of view of 280 μrad, which is equal to the satellites location uncertainty projected onto the sky. During the acquisition process, after the space terminal detects the beacon beams it will point to the ground station and transmit its downlink beam. This will be detected by the acquisition camera and will be used to bring the space terminals beam to the center of the WFS field of view, which can then close the AO loop.

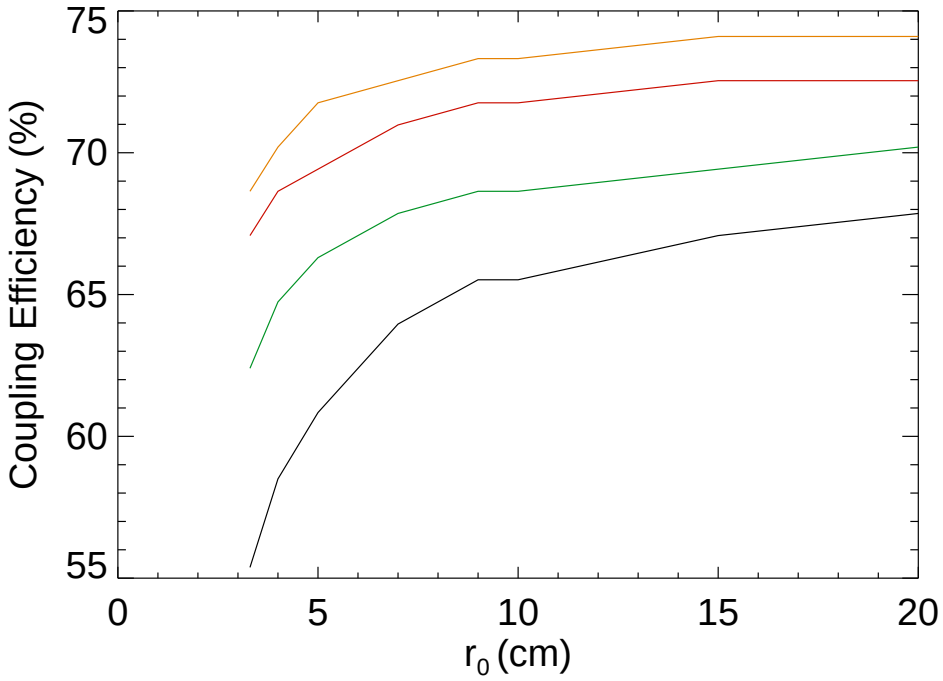

Figure 2. The coupling efficiency as a function of turbulence conditions as measured by the Fried's parameter, r_0. The different curves correspond to increasing elevation angle. The black curve is for 20°, the green curve is for 30°, the red curve is for 40° and the orange curve is for 50°.

The transmit system also relays the communication beam from the laser amplifier to the telescope with a beam divergence of 20 μrad at a wavelength of 1563 nm. The transmit laser has an average power of 10 W. The transmit beam is pointed 18 μrad off axis of the optical axis of the telescope to account for the light travel time between the two terminals. The AO system is seeing on-axis light, while the transmitted communication beam is slightly off axis.

One challenge for the IOS design is the uplink lasers are on the order of tens of Watts of power, while the WFS in the receive system is sensitive to nanoWatts of power. Both systems are mounted on the same optical bench. The 10^{10} ratio in intensity between the two sides requires that we prevent any of the scattered light from the transmit system from entering the WFS. While the uplink beams are at different wavelength from the downlink beam, the AO system's WFS camera is sensitive to light from 1.0-1.7 μm and will detect any transmit light that gets to it. A similar concern is amplified spontaneous emission (ASE) from the uplink lasers. ASE causes fiber amplified lasers to emit light at wavelengths other than the desired wavelength. This light also has to be stopped from entering the receive path. Both scattered light and ASE will be prevented from entering the WFS through the use of narrow-band filters and baffles. These will also reduce the amount of sky background that gets to the WFS.

The majority of the transmit system optics are located on a separate breadboard that will be mounted on the optical table in the OCTL lab. Each of the beacon lasers and the communication laser have integral collimators mounted at the end of their fiber. These are held in place in a custom mount. From here the beams are reflected off of three steering mirrors. The steering mirrors are arranged so that they have approximately the same path length and that the indvidual beams are brought back together and have a common focus point. The communication beam goes through a lens to adjust the divergence relative to the beacon beams. This is the only optic that differs between the beacon and communication arms. After the beam steering mirrors, the beams leave the breadboard and encounter a lens that adjusts the beams so they have the proper divergence. Then the

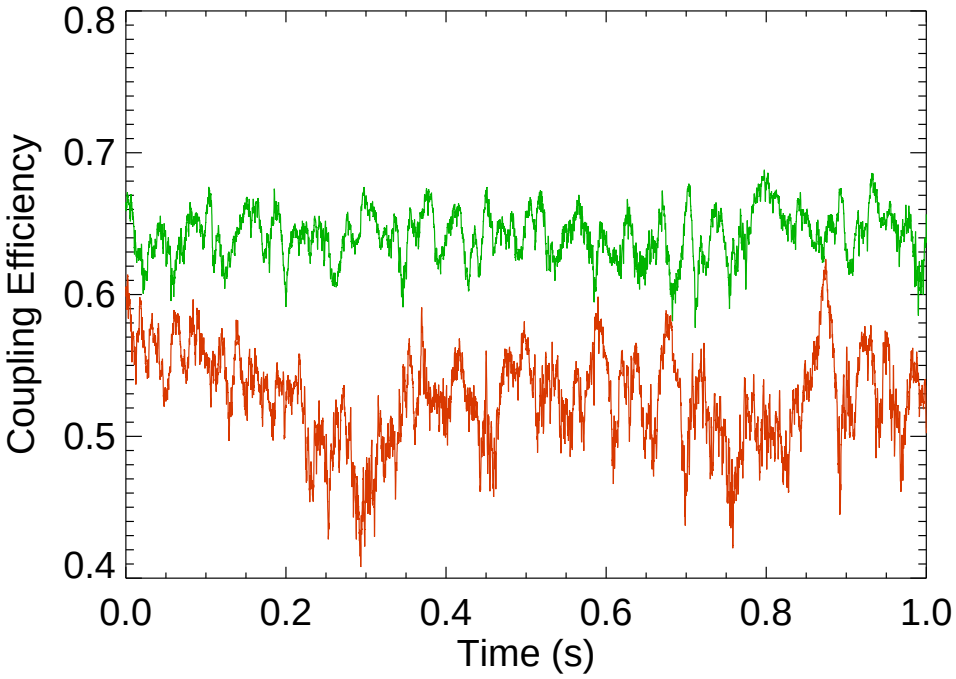

Figure 3. The time series of coupling efficiency for an elevation of 20°. The green curve is the coupling for the nominal conditions, while the red curve is for the 90% conditions. The nominal conditions have an average value of 0.64 with a standard deviation of 0.0174, while the 90th percentile conditions have an average coupling of 0.53 with a standard deviation of 0.0331.

beams encounter a fold flat to stay on the table, a Dove prism so the beam pattern can be adjusted to avoid telescope spiders and then another lens that adjusts the focus of the beams. After this the beams pass through the laser safety shutter, two more fold flats and then finally they reflect off the transmit/receiver dichroic. They then go through a periscope that is used to adjust the beam height and angle.

Figure 4 shows the beam footprints at the pupil of the telescope. This foot print propogates to orbit so that it forms the beam profile shown in Figure 5

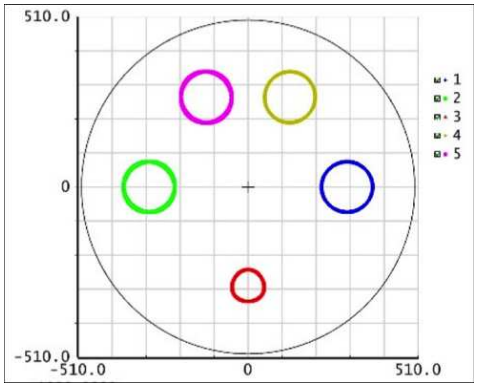

Figure 4. The beam footprint at the pupil of the telescope.

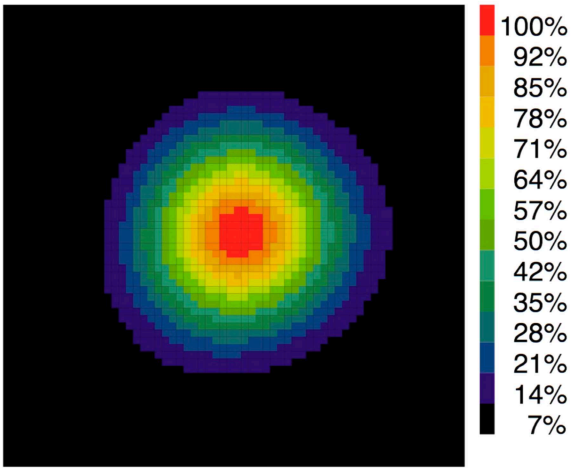

Figure 5. The simulated beacon beam profile on orbit.

4. SOFTWARE ARCHITECTURE

The IOS software is based on the PALM-3000 software design.[13] Where functionally possible, existing PALM-3000 software was reused. We estimate that we have reused approximately 50% of the PALM-3000 code; this was a great time saver. Also, the IOS software is effectively a second generation version of the PALM-3000 code; this provides opportunities to incorporate lessons learned and to improve on the existing code.

The system design is divided into four main components: a command/automation server, a device driver server, the real-time control component, and the graphical user interface running on a computer in the operators room. The publish/subscribe communication method is used to transfer messages between components, a particularly effective method for systems with components running in physically separate locations. The real-time component uses a Digital Signal Processor (DSP) board with eight on-board DSP chips. We use direct memory access (DMA) to get data from the frame grabber directly to the DSP board enabling us to achieve the required frame rates. All published data is written to the database in the form of commands, status messages, and telemetry data. A separate component acts as the interface to the database; a slightly enhanced version of the Berkeley DB database engine. A solid state drive in the IOS control computer is capable of capturing all of telemetry data types at the highest possible log rates. This will enable us to analyze performance during testing and operations.

Graphic Processor Units (GPU) based systems have become the standard for low latency AO real-time control systems.[14,15] While GPU systems are able to meet latency requirements of many instruments in operation today, they are limited in their processing capability by two factors: the lack of GPU support for application-level direct access to PCI Express and the absence of frame grabbers with application-tuned direct memory access (DMA) transfer size capability. IOS has solved this problem by using a multi-DSP based real-time control system that leverages the PCI Express multicast capability and a DMA-tuned frame grabber.

As the WFS takes an image it is captured by the frame grabber. From the frame grabber, the image is read out row by row. When there are two rows of data available, it gets shipped to the DSP board. Each of the eight DSP chips on the board contains eight cores. Each of the 64 cores measures the centroids of all the lenslets, but each core is assigned specific DM Actuators to compute the commands for. When the commands are computed, the DMA controller on each DSP chip transfers the DM commands to the appropriate DM via DMA. All of the above steps are done via DMA, which bypasses the central processing unit (CPU) and eliminates the CPU

timing jitter. This enables us to deliver processing rates in excess of 20 kHz and a latency in the single-digit microsecond range for 56×64 pixel frames.

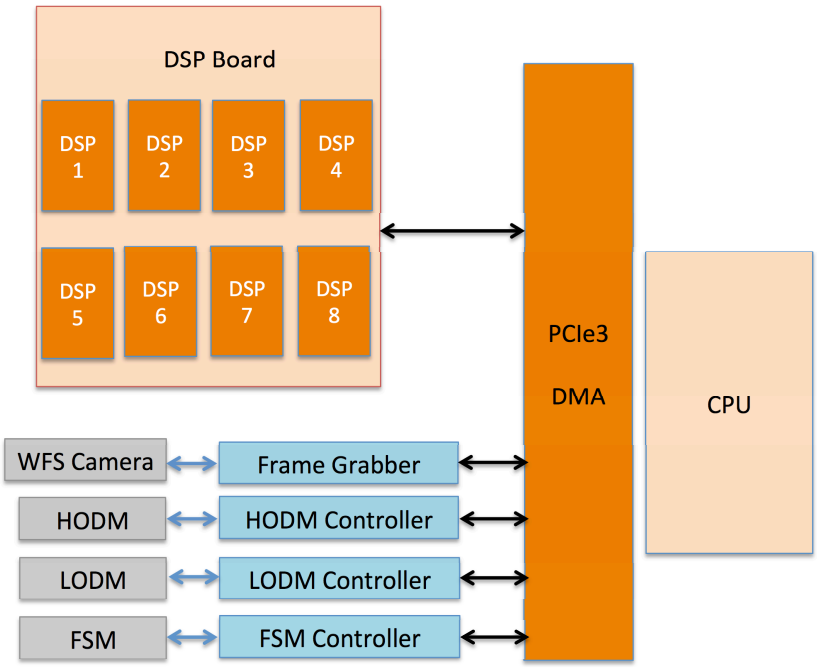

Figure 6. Data are exchanged between the frame grabber, the DSP card and the active mirror elements via DMA, without going through the CPU, which would add timing jitter and increase the control loop latency, leading to degraded performance.

5. STATUS AND FUTURE OF IOS

The IOS has successfully passed its Critical Design Review and is now in integration. The AO system is undergoing final alignment. In the coming months, we will test the hardware with the real-time control system. This will allow us to fully optimize the real time system. At the beginning of 2017, we will start the alignment of the beam corral portion of the transmit system. This will be tested with a single beacon laser. In late 2017, we will move the IOS to the OCTL telescope, where it will be assembled as a single instrument for the first time. It will then undergo integration and testing with the OCTL facility and over time with the rest of the OGS1 system as they are delivered to OCTL. During this period, we will be testing the IOS AO system on stars observing through broadband filters. At the end of the testing period, we Will switch the broadband filters for narrow band filters so that the system can be used with the downlink laser. The mission is scheduled to launch in early 2019.

6. SUMMARY

When operational, the IOS system will be capable of achieving coupling efficiency's of greater than 50% in nominal atmospheric conditions at Table Mountain in California during daytime and nighttime. The IOS will also transmit the communication and beacon beams with the proper divergences to allow the space terminal to acquire the ground station and commence the communication link. It will be a key enabling system for the LCRD project and will enable us to better understand how to build future ground stations.

7. ACKNOWLEDGMENTS

The research was carried out at the Jet Propulsion Laboratory, California Institute of Technology, under a contract with the National Aeronautics and Space Administration (NASA).

REFERENCES

[1] Luzhansky, E., Edwards, B., Israel, D., Cornwell, D., Staren, J., Cummings, N., Roberts, T., and Patschke, R., "Overview and status of the Laser Communication Relay Demonstration," in [*Free-Space Laser Communication and Atmospheric Propagation XXVIII*], Hemmati, H. and Boroson, D. M., eds., *Proc. SPIE* **9739**, 97390C–1 (2016).

[2] Edwards, B. L., Israel, D., Wilson, K., Moores, J., and Fletcher, A., "Overview of the Laser Communications Relay Demonstration project," *Proc. of the International Conference of Space Operations* , 1261897 (2011).

[3] Roberts, W. T., Antsos, D., Croonquist, A., Piazzolla, S., Roberts, L. C., Garkanian, V., Trinh, T., Wright, M. W., Rogalin, R., Wu, J., and Clare, L., "Overview of Optical Ground Station 1 of the NASA Space Communications and Navigation Program," in [*Free-Space Laser Communication and Atmospheric Propagation XXVIII*], Hemmati, H. and Boroson, D. M., eds., *Proc. SPIE* **9739**, 97390B–1 (2016).

[4] Wilson, K., Britcliffe, M., and Golshan, N., "Progress in design and construction of the Optical Communications Telescope Laboratory (OCTL)," in [*Free-Space Laser Communication Technologies XII*], Mecherle;, G., ed., *Proc. SPIE* **3932**, 112–116 (2000).

[5] Edwards, B. L., Robinson, B., Biswas, A., and Hamkins, J., "An overview of nasas latest efforts in optical communications," *ICSOS* , 1–8 (2015).

[6] Wallace, J. K., Crawford, S., Loya, F., and Moore, J., "A phase-shifting zernike wavefront sensor for the palomar P3K adaptive optics system," *Proc. SPIE* **8447**, 84472K (2012).

[7] Rhoadarmer, T. A. and Barchers, J. D., "Noise analysis for complex field estimation using a self-referencing interferometer wave front sensor," *Proc. SPIE* **4825**, 215–227 (2008).

[8] Bifano, T., "Shaping light: MOEMS deformable mirrors for microscopes and telescopes," *Proc. SPIE* **7595**, 759502 (2010).

[9] Mantravadi, S., Rhoadarmer, T., and Glas, R., "Simple laboratory system for generating well-controlled atmospheric-like turbulence," in [*Advanced Wavefront Control: Methods, Devices, and Applications II*], Gonglewski, J., Gruneisen, M. T., and Giles, M. K., eds., *Proc. SPIE* **5553**, 290–300 (2004).

[10] Burruss, R., Serabyn, E., Mawet, D., Roberts, J., Hickey, J., Rykoski, K., Bikkannavar, S., and Crepp, J., "Demonstration of on sky contrast improvement using the modified Gerchberg-Saxton algorithm at the Palomar Observatory," in [*Free-Space Laser Communication and Atmospheric Propagation XXVIII*], Ellerbroek, B., Hart, M., Hubin, N., and Wizinowich, P. L., eds., *Proc. SPIE* **7736**, 77365X (2010).

[11] Hardy, J., [*Adaptive Optics*], Oxford University Press, New York, NY (1998).

[12] Roberts, L. C. and Bradford, L. W., "Improved models of upper-level wind for several astronomical observatories,," *Opt. Express* **19**, 820–837 (2011).

[13] Truong, T. N., Bouchez, A. H., Burruss, R. S., Dekany, R. G., Guiwits, S. R., Roberts, J. E., Shelton, J. C., and Troy, M., "Design and implementation of the PALM-3000 real-time control system," *Proc. SPIE* **8447**, 844702F (2012).

[14] Dekany, R., Roberts, J., Burruss, R., Bouchez, A., Truong, T., Baranec, C., Guiwits, S., Hale, D., Angione, J., Trinh, T., , J. Z., Shelton, J. C., Palmer, D., Henning, J., Croner, E., Troy, M., McKenna, D., Tesch, J., Hildebrandt, S., and Milburn, J., "PALM-3000: Exoplanet adaptive optics for the 5 m Hale telescope," *ApJ* **776**, 130 (2013).

[15] Sevin, A., Perret, D., Gratadour, D., Lainé, M., Brulé, J., and Ruyet, B. L., "Enabling technologies for GPU driven adaptive optics real-time control," *Proc. SPIE* **9148**, 91482G (2014).